Lidija Ćurković[1], Ivana Ropuš[2], Irena Žmak[1], Ivana Gabelica[1], Zrinka Švagelj[1]

Comparison of Mechanical Properties of Conventionally and Non-Conventionally Sintered Cold Isostatically Pressed Al_2O_3 Ceramics

[1] Faculty of Mechanical Engineering and Naval Architecture, University of Zagreb, I. Lučića 1, 10000 Zagreb, Croatia
[2] Energoatest zaštita d.o.o., Potočnjakova 4, 10000 Zagreb, Croatia

Abstract

The objective of this study was to investigate and compare the morphology and mechanical properties of cold isostatically pressed (CIP) alumina (Al_2O_3) samples sintered by conventional (electrical) and non-conventional (hybrid microwave) techniques. Scanning electron microscopy (SEM) was used to examine the morphology of the Al_2O_3 ceramics sintered by both sintering techniques. Following mechanical properties of CIP alumina ceramics were analysed: (i) Vickers hardness, (ii) Vickers indentation fracture toughness (VIF), (iii) the indentation size effect (ISE) using Vickers method, and (iv) the brittleness index. The ISE is analysed using (i) the Meyer's law, (ii) the proportional specimen resistance (PSR) model, and (iii) the modified proportional specimen resistance (MPSR) model. It was found that alumina samples sintered in the electric kiln obtained higher density and lower porosity compared to the samples sintered in the hybrid-microwave kiln. The obtained values of the Meyer's index n are less than 2 for alumina ceramics sintered by both sintering methods, which indicates that the hardness is dependent on the test load. High correlation coefficients confirm that all applied mathematical models are suitable. However, true Vickers hardness obtained by the PSR model was found to be nearer to the measured Vickers hardness of alumina samples regardless of the sintering method applied. Furthermore, it was found that the fracture toughness was higher for alumina ceramics sintered in the hybrid microwave kiln (MK-Al_2O_3) than the one sintered in the electric kiln (EK-Al_2O_3). In contrary, the brittleness index was found to be higher for alumina ceramics sintered in the electric kiln (EK-Al_2O_3) than in the hybrid microwave kiln (MK-Al_2O_3). Both Vickers hardness and brittleness index values might be correlated to the microstructure of the sintered samples, e.g. finer for non-conventionally sintered alumina.

Keywords: *alumina ceramics, sintering, mechanical properties.*

1. Introduction

Each step of the ceramic production process: (i) the selection of raw materials and additives, (ii) the forming of the green bodies, and (iii) the sintering process have an important impact on the microstructure, and thereby the desired properties of the final ceramic product [1,2]. Sintering, as a final step in the ceramics production, may be conducted either by a conventional or non-conventional sintering method. The main goal of the sintering

process is to achieve full densification of the material, with the density as near as the theoretical density values as possible. Also, the sintering process can be used to obtain porous materials with high surface area. In this case, full consolidation is not reached.

The sintering of ceramic materials is an energy-consuming process with high production costs. To optimize the sintering process, densification mechanisms can be modified to improve the microstructure and mechanical properties of the obtained sintered ceramic materials as well as to reduce the production time and costs [1]. Therefore, emerging new techniques of sintering, such as spark plasma and microwave sintering are continuously being improved and applied. Microwave-assisted sintering, as one of the non-conventional sintering methods, was developed to reduce the energy consumption, maintain or improve the characteristics of the resulting ceramics, as well as to reduce the production costs and lessen environmental impact. With the microwave sintering method, highly dense materials can be obtained by rapid (>400 °C/min) and volumetric heating without substantial grain broadening because the processing times are considerably shorter than in conventional sintering [2,3]. The difference between the conventional and non-conventional sintering processes is in the heat transfer. Conventional sintering includes heat transfer via conduction from the outside to the inside of the sintered material, while the microwave heating process generates heat internally, i.e., within the sintered material and is transmitted outwards (Figure 1). The conventional sintering is based on conventional heat transfer mechanisms: conduction, convection, and radiation [3-5].

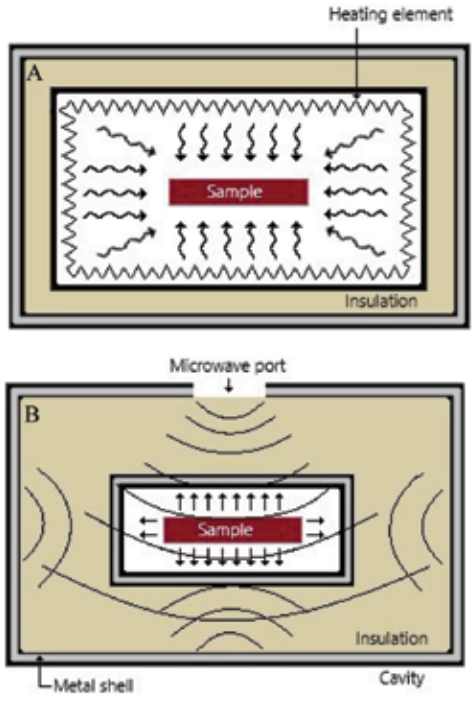

Fig. 1. Heating patterns in: (A) conventional furnace and (B) microwave furnace [4,5].

The interaction of microwaves with different materials depends on the electrical and magnetic properties of the material as well as on the grain size and porosity. Regarding these properties, materials can be classified as transparent (no energy transfer – low dielectric loss materials), opaque (no penetration into the material – bulk materials, conductors), and absorbent (absorption and exchange of energy – high dielectric loss materials), as shown in Figure 2.

Microwave sintering can be used for the preparation of different engineering materials: (i) ceramics, such as barium calcium zirconate titanate [7], magnesium aluminate spinel [8], yttria-tetragonal zirconia [9], high density yttria and lanthana co-doped zirconia dioxide [10], magnesium oxide doped alumina [11], Al_2O_3–yttria-stabilized ZrO_2 [12], alumina [13], β-SiC [14], (ii) metals and alloys, such as Ti-3Cu alloys [15], stainless steel 316L (X2CrNiMo17-12-2) [16], Cu–Sn bronze [17], FeCuCo metallic matrix [18], (iii) composites, for example Al_2O_3–SiC ceramic composites [19], W-30Cu composites [20], zirconia nanocomposite powders doped with ceria and toughened with alumina [21], boronised Ti6Al4V/HA composite [22], etc.

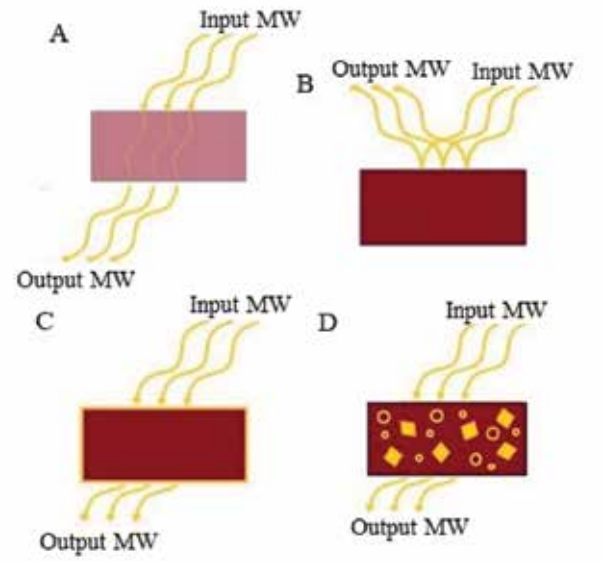

Fig. 2. Schematic diagram illustrating the interactions of microwaves with: (A) transparent material (low loss insulator) – total penetration, (B) opaque material (conductor) – no penetration, (C) absorber (lossy insulator) – partial to total penetration, and (D) absorber (mixed) –matrix is transparent, but fibres, particles or additives in matrix are absorbing materials – partial to total penetration [6].

Mechanical properties of the ceramic materials are strongly influenced by the degree of densification. Hardness, as one of the important mechanical properties of ceramic materials, represents material's resistance to plastic deformation. For testing very hard materials, such as ceramics, it is commonly used Vickers (*HV*) or Knoop (*HK*) method, because their diamond pyramidal penetrators can leave visible indentations. The value of

the applied load, used during the hardness testing, can influence the testing results [23]. The change in applied load causes changes in manifested ("apparent") hardness. The phenomenon when the hardness decreases with the increasing load (Meyer's number $n < 2$, Figure 3) is called normal indentation size effect (ISE) [24-28]. It is also possible that the material manifests an increase in hardness with increasing indentation load (Meyer's number $n > 2$, Figure 3), which is known as reverse ISE (RISE) [23,28,29]. Figure 3 illustrates non-constant or load dependent hardness ("apparent" hardness), and constant hardness ("true" hardness or load-independent hardness), which usually occurs at higher indentation loads [23,28].

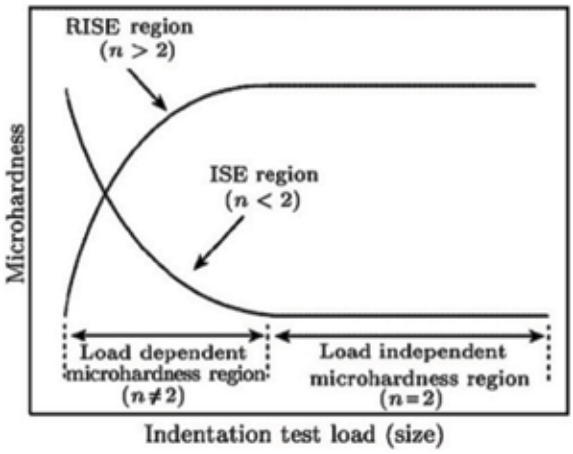

Fig. 3. Schematic plot of hardness variation with test load, showing the indentation size effect (ISE) and reverse indentation size effect (RISE) [23,28].

In this research, the morphology and the mechanical properties (Vickers hardness, Vickers indentation fracture toughness, the indentation size effect (ISE) using Vickers method, and the brittleness index) of cold isostatically pressed Al_2O_3 samples sintered by conventional (electric) and non-conventional (hybrid microwave) techniques were determined and compared. The observed ISE of alumina ceramics sintered in the electric and hybrid microwave kiln was analysed using the traditional Meyer's law, the proportional specimen resistance (PSR) model, and the modified proportional specimen resistance (MPSR) model.

Hybrid microwave heating was applied because the microwave-assisted sintered material distributes the temperature field more evenly, thus achieving a more uniform heating throughout the cross-section of the material (Figure 4) and, consequently avoiding the density gradient.

Due to this more uniform heating, alumina ceramics with a more homogeneous and fine-grained microstructure, and therefore improved final properties, can be obtained.

2. Materials and methods

High purity Al_2O_3 powder (Alteo, France) was used in this research as raw alumina powder for the preparation of alumina granules by spray drying. The chemical composition of the raw alumina powder according to manufacturer's declaration is listed in Table 1. According to the results of the chemical composition analysis, raw Al_2O_3 powder has a high purity of 99.83 wt. %. The presence of MgO as a sintering aid and the following impurities: CaO, Fe_2O_3, Na_2O and SiO_2 were also confirmed.

Table 1. Chemical composition of raw Al_2O_3 powder.

Sample	wt. %					
	CaO	Fe_2O_3	MgO	Na_2O	SiO_2	Al_2O_3
Al_2O_3 powder	0.0200	0.0180	0.0450	0.0500	0.0325	balance

Cold isostatic pressed (CIP) cylindrical pellets produced at Applied ceramics, Croatia, of high-purity Al_2O_3 ceramics with a diameter of 10 mm and a height of 20 mm were used in this research.

The cylindrical alumina pellets, used for the study of the conventional sintering method (samples "EK"), were sintered using an electric kiln (Nabertherm P310, Germany) at 1600 °C for 6 h. The second cylindrical pellet set (samples "MK") were sintered by the non-conventional sintering method in a hybrid microwave kiln (Over, Kerestinec, Croatia) at 1600 °C for 1 h. The sintering regimes were adopted according to the preliminary results [31].

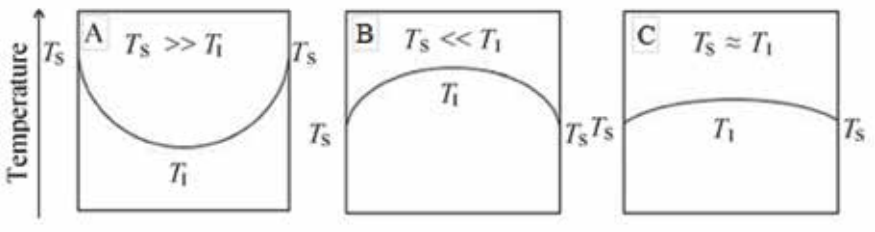

Fig. 4. Temperature distribution in ceramic material heated by: (A) conventional, (B) microwave, and (C) hybrid heating (T_s – surface temperature; T_I – internal temperature) [5,30].

The hybrid microwave kiln used a low-frequency (2.45 GHz) and 1.5 kW microwave magnetron. A silicon carbide susceptor was used to aid the heating of the sample in the microwave cavity.

The density of all sintered samples was determined according to the Archimedes' method using analytical balance Ohaus AP250D (Ohaus, Florham Park, NJ, USA).

The morphology of the fracture surface of the samples sintered by both techniques was analysed by the scanning electron microscope (SEM) TS5136LS (Tescan Vega, Brno, Czech Republic).

Prior to the measurements of Vickers hardness, the samples were prepared by the standard ceramographic technique [32]. Hardness tester Wilson Wolpert Tukon 2100B (*HV*0.1 – *HV*1) (Instron, Grove City, PA, USA) and Vickers tester Zwick (*HV*3 and *HV*5) were used for hardness measurement. Diagonals were measured on the optical microscope Olympus BH (Olympus Imaging Corp., Tokyo, Japan) immediately after unloading. The Vickers hardness was measured 10 times per sample under the loads listed in Table 2 at room temperature.

Table 2. Loads used for Vickers hardness testing.

F, N	*HV*
0.9807	*HV*0.1
2.942	*HV*0.3
4.903	*HV*0.5
9.807	*HV*1
29.42	*HV*3
49.03	*HV*5

The Vickers hardness was calculated according to the following equation [28]:

$$HV = \alpha \frac{F}{d^2} \quad (1)$$

where F stands for the applied load (N), d (mm) is the mean value of the indentation diagonals (Equation 2) [28], while α is the indenter's geometrical constant, i.e. 0.1891 for the Vickers diamond pyramid.

$$d = \frac{d_1 + d_2}{2} \quad (2)$$

Fracture toughness for alumina ceramics sintered by both sintering methods was determined by the Vickers indentation fracture (VIF) or Vickers indentation crack length method. This method uses the Vickers indenter to make the hardness indentation on a polished ceramic sample surface. The indenter creates a plastically deformed area underneath the indenter as well as cracks that emanate radially outward and downward from the vertices of the Vickers indentation.

Two types of cracks can occur: (i) radial-median cracks and (ii) Palmqvist cracks (Figure 5). A simple way to differentiate between the two types is to polish the surface layers away: the median crack system will always remain connected to the inverted pyramid of the indentation, while the Palmqvist cracks will become detached, as shown in Figure 5.

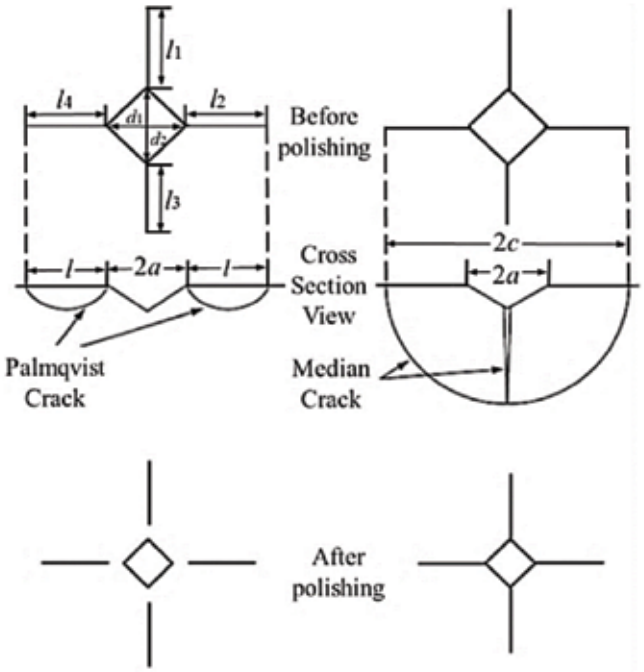

Fig. 5. Palmqvist and median crack system developed from the Vickers indents, before and after polishing [31].

A second way to distinguish the crack system present in the analysed material consists of the determination of *c/a* ratio (*c* is the crack length from the centre of the indent to the crack tip, and *a* is the half value of the indentation diagonal, Figure 5). If it is less than 2.5, then the material shows Palmqvist crack system, while for median cracks system values of *c/a* is higher than 2.5 [31]. The obtained values of *c/a* (for *HV*1) were 2.16 ± 0.26, and 1.81 ± 0.31 for alumina ceramics sintered in the electric and hybrid microwave kiln, respectively. The obtained values of *c/a* indicate that Palmqvist crack was present in both alumina ceramic samples. Therefore, three equations based on the Palmqvist crack were found to be applicable for the fracture toughness determination of the alumina ceramic samples (Table 3).

Table 3. Equations for the calculation of Vickers indentation fracture toughness (K_{IC}) values for Palmqvist crack type.

Equations	Authors
$K_{Ic} = 0.024 \cdot \frac{F}{c^{1.5}} \cdot \left(\frac{E}{HV}\right)^{0.5}$	Casellas [33]
$K_{Ic} = 0.0319 \cdot \frac{F}{a \cdot l^{0.5}}$	Shetty et al. [34]
$K_{Ic} = 0.0089 \cdot \left(\frac{E}{HV}\right)^{0.4} \cdot \frac{F}{a \cdot l^{0.5}}$ for $0.25 < l/a < 2.5$	Niihara et al. [34]

F, load applied during Vickers test (N); c, the crack length from the centre of the indentation to the crack tip (m); E, Young's modulus (GPa); HV, the Vickers hardness (GPa); l, the crack length measured from vertices of the indentation to the crack tip (m); a, half of the indentation diagonal (m).

3. Results and discussion

The SEM images of the microstructure of the ceramic fracture surface sintered by conventional (electric kiln) and non-conventional (hybrid microwave kiln) methods are shown in Figure 6.

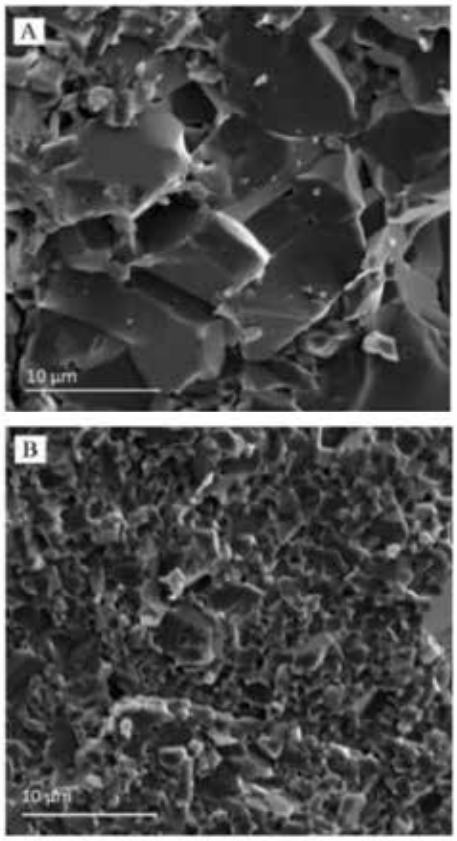

Fig. 6. SEM images of the fracture surface of Al_2O_3 ceramics sintered by (A) conventional (electric kiln) and (B) non-conventional (hybrid microwave kiln) sintering with the same magnification of 4500 times.

The most distinctive change was the grain size. Finer grain size was obtained for alumina samples sintered by the hybrid microwave kiln (non-conventional sintering method), where the process took less time and was more energy efficient.

The relative density of alumina ceramic sintered by conventional and non-conventional methods is 96.9 % ± 0.5 % and 94.9 % ± 0.7 %, respectively.

The porosity of alumina ceramic sintered by conventional and non-conventional methods is 3.1 % ± 0.5 % and 5.1 % ± 0.7 %, respectively.

The samples sintered in the electric kiln achieved a higher density and less porosity compared to the samples sintered in the hybrid-microwave kiln.

The value of Vickers hardness (HV) for different applied indentation load are presented in Figure 7.

The results show that the hardness decreases with the increasing indentation test load. The presented data on the dependence of the hardness on the applied load confirm the indentation size effect (ISE). The observed decrease in hardness with the increasing load is the normal ISE. All data shown in Figure are averages values of ten measurements.

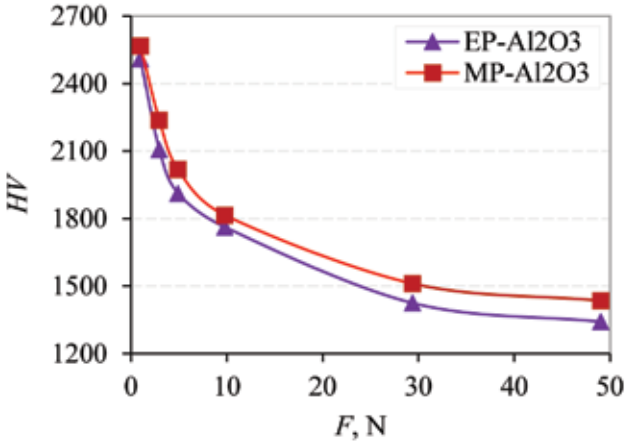

Fig. 7. Dependence of measured Vickers hardness on applied load for alumina ceramics sintered in (A) electric kiln (EK-Al_2O_3) and (B) hybrid microwave kiln (MK-Al_2O_3).

To quantify the normal indentation size effect (ISE), three models were applied to the obtained data: Meyer's law, the proportional specimen resistance (PSR) and the modified proportional specimen resistance (MPSR) model.

Meyer's law gives the relation between the applied load, F, and the average value of the indentation diagonals, d, according to Equation 3 [35].

$$F = K \cdot d^n \quad (3)$$

where n represents the Meyer's number (index), and K is the standard hardness constant for a given material. The

Equation 3 coefficients can be obtained by linear regression analysis from the log F versus log d plots (Figure 8), where the slope represents the Meyer's index, while the intercept gives log K values. These coefficients are shown in Figure 8 and listed in Table 4.

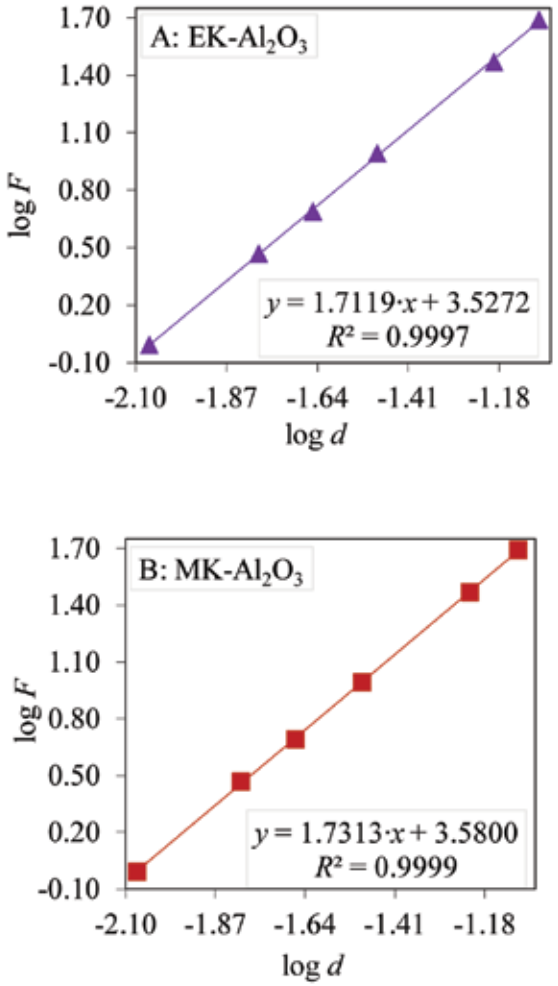

Fig. 8. Vickers hardness data for alumina ceramics sintered in (A) electric kiln (EK-Al_2O_3) and (B) hybrid microwave kiln (MK-Al_2O_3) according to Meyer's law

Table 4. Results of Vickers hardness data analysis according to Meyer's law for alumina ceramics sintered in the electric kiln (EK-Al_2O_3) and hybrid microwave kiln (MK-Al_2O_3).

Parameter	Sample	
	EK-Al_2O_3	MK-Al_2O_3
n	1.7119 ± 0.0228	1.7313 ± 0.0332
log K	3.5272 ± 0.0361	3.5800 ± 0.0526
K (N·mm^{-n})	2718	3619
R^2	0.9997	0.9999

The proportional specimen resistance (PSR) model is a modification of the Meyer's law [36], a modification that explains the relationship between the applied load, F, and the indentation diagonal, d, considering the energy balance. PSR is described by Equation 4:

$$F = a_1 \cdot d + a_2 \cdot d^2 \quad (4)$$

where a_1 (N·mm^{-1}) is a constant related to the specimen resistance representing the energy used to create new surfaces or the energy used in friction and elastic deformations. Coefficient a_2 (N·mm^{-2}) is a measure of the "true" hardness, meaning the hardness that is load independent and is related to permanent deformation [28,35]. These coefficients are shown in Figure 9 and listed in Table 5.

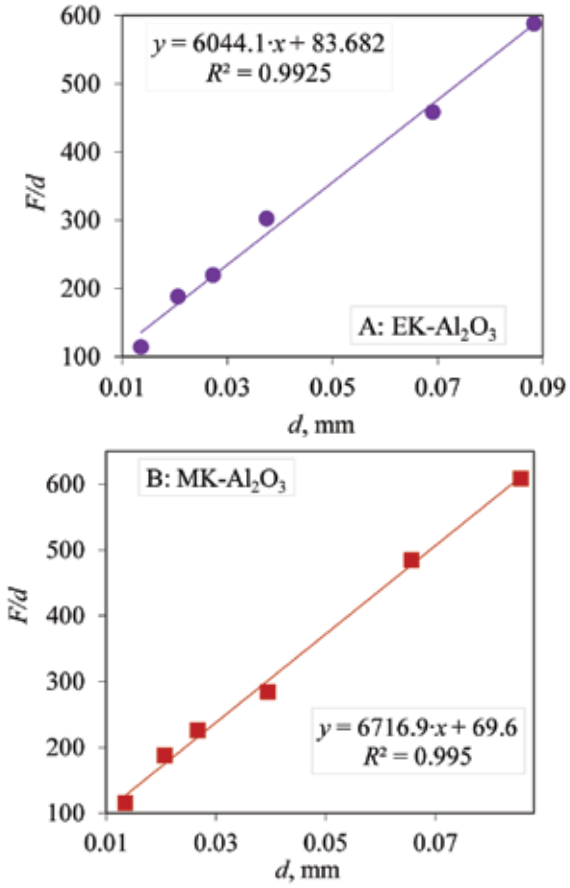

Fig. 9. Vickers hardness data for alumina ceramics sintered in (A) electric kiln (EK-Al_2O_3) and (B) hybrid microwave kiln (MK-Al_2O_3) according to proportional specimen resistance (PSR) model.

Modified proportional specimen resistance (MPSR) model is an expanded PSR model with an additional coefficient, a_0 (N) related to the material properties and the quality of sample surface preparation. MPSR model is expressed by Equation 5 [28,37].

$$F = a_0 + a_1 \cdot d + a_2 \cdot d^2 \quad (5)$$

The coefficients (a_2, a_1 and a_0.) of the obtained curves are presented in Table 6 and shown in Figure 10. The

coefficients obtained by polynomial regression analysis of the F versus d plot are presented in Table 6.

Table 5. Regression analysis results of experimental Vickers hardness data, according to proportional specimen resistance (PSR) model for alumina ceramics sintered in the electric kiln (EK-Al_2O_3), and hybrid microwave kiln (MK-Al_2O_3).

Parameter	Sample	
	EK-Al_2O_3	MK-Al_2O_3
a_1, N·mm^{-1}	83.7 ± 9.8872	69.9 ± 12.174
a_2, N·mm^{-2}	6044 ± 262	6717 ± 220
R^2	0.9925	0.9950

Table 6. Regression analysis results of experimental Vickers hardness data according to the modified proportional specimen resistance (MPSR) model for alumina ceramics sintered in (A) electric kiln (EK-Al_2O_3) and (B) hybrid microwave kiln (MK-Al_2O_3).

Parameter	Sample	
	EK-Al_2O_3	MK-Al_2O_3
a_0, N	0.058 ± 0.812	−0.019 ± 0.635
a_1, N·mm^{-1}	87 ± 49	72 ± 38
a_2, N·mm^{-2}	5963 ± 518	6691 ± 421
R^2	0.999	0.999

The residual surface stress coefficients a_0 reach relatively small values due to the careful grinding and polishing of the specimens.

"True" Vickers hardness HV_T can be calculated according to Equation 6 [28,37]:

$$HV_T = \alpha \cdot a_2 \quad (6)$$

where α is the geometrical constant of the indenter (0.1891 for Vickers), and a_2 is the coefficient of the PSR and MPSR models, related to the occurred permanent deformation. "True" Vickers hardness values of the sintered Al_2O_3 ceramics in the electric and hybrid microwave kiln are summarized in Table 7.

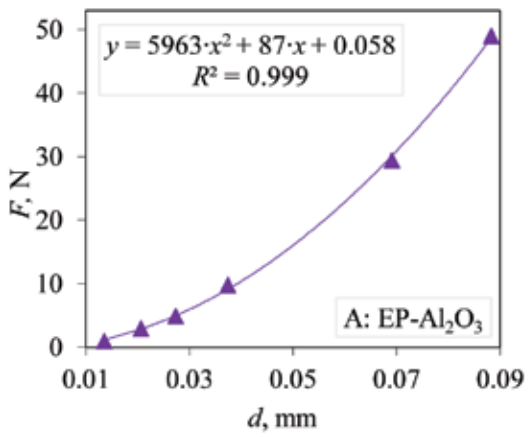

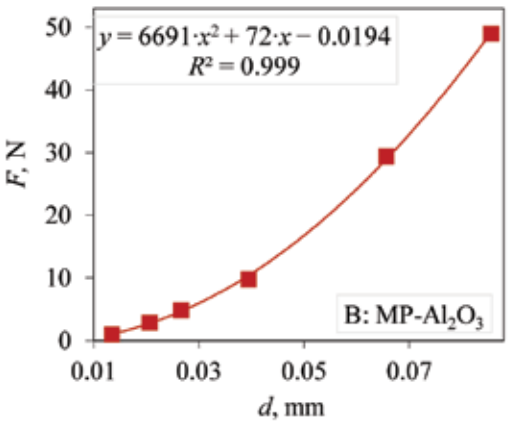

Fig. 10. The Vickers hardness data for alumina ceramics sintered in (A) electric kiln (EK-Al_2O_3) and (B) hybrid microwave kiln (MK-Al_2O_3) according to the modified proportional specimen resistance (MPSR) model.

Table 7. "True" Vickers hardness values of alumina ceramics sintered in the electric kiln (EK-Al_2O_3) and hybrid microwave kiln (MK-Al_2O_3), according to PSR and MPSR models.

Model	Sample	
	EK-Al_2O_3	MK-Al_2O_3
PSR	1143	1270
MPSR	1128	1265

The "true" values determined by PSR and MPSR models show an 11 % to 12 % higher hardness of the samples sintered in the hybrid microwave kiln (MK-Al_2O_3), compared to the samples sintered in the electric kiln (EK-Al_2O_3).

After measuring the alumina ceramics hardness by the Vickers indentation method, the lengths of cracks induced in the process were used to calculate the Vickers indentation fracture toughness (K_{Ic}) according to three chosen models (Table 3) for the Palmqvist crack type. The obtained results of the Vickers indentation fracture toughness for both alumina samples are presented in Figure 11.

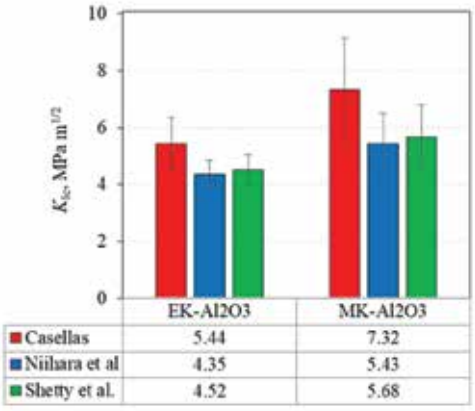

Fig. 11. Comparison of Vickers indentation fracture toughness values for alumina ceramics sintered in the electric kiln (EK-Al_2O_3), and (B) hybrid microwave kiln (MK-Al_2O_3) for Palmqvist crack type.

All applied models showed that the fracture toughness is higher for alumina ceramics sintered in the hybrid microwave kiln (MK-Al_2O_3) than in the electric kiln (EK-Al_2O_3).

For both alumina samples, the brittleness index (B_i, $\mu m^{-1/2}$) was calculated by the ratio of Vickers hardness ($HV1$, GPa), and the Vickers indentation fracture toughness (K_{IC}, $MPa \cdot m^{1/2}$) using the following equation [31,39]:

$$B_i = \frac{HV}{K_{IC}} \quad (7)$$

The calculated values of the brittleness index (B_i, $\mu m^{-1/2}$) for both sintered samples are shown in Figure 12. All models showed that the value of brittleness index is higher for alumina ceramics sintered in the electric kiln (EK-Al_2O_3) than in the hybrid microwave kiln (MK-Al_2O_3).

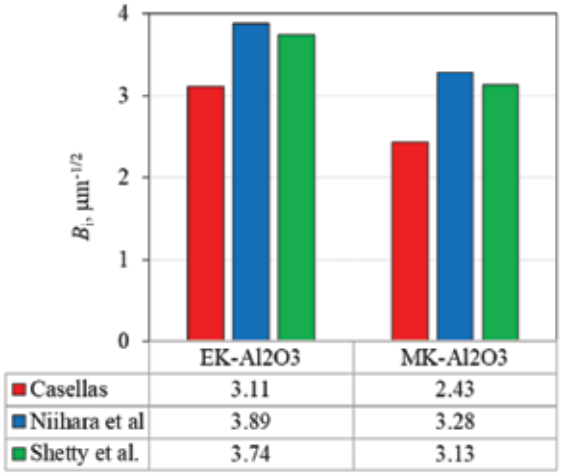

Fig. 12. Brittleness index (B_i, $\mu m^{-1/2}$) values for Palmqvist crack type.

4. Conclusions

The results presented in this paper may be summarized as follows:

- It was found that Al_2O_3 ceramics sintered in the electric kiln achieved a higher density and lower porosity, compared to the samples sintered in the hybrid-microwave kiln.
- The measured hardness of conventionally and non-conventionally sintered Al_2O_3 ceramics decreases with an increase in applied indentation load, meaning that both materials undergo the normal indentation size effect.
- Three different mathematical models were used for the analysis of the normal indentation size effect: the Meyer's law, the proportional specimen resistance (PSR) and the modified proportional specimen resistance (MPSR) model. Meyer's indexes were less than 2 for both samples: 1.7119 for the samples sintered in the electric kiln, and 1.7313 for the samples sintered in the hybrid microwave kiln, which also confirmed the normal indentation size effect.
- The samples sintered in the hybrid microwave kiln have a higher "true" Vickers hardness possibly due to the finer microstructure, compared to conventionally sintered alumina samples.
- The fracture toughness (K_{IC}, $MPa \cdot m^{1/2}$) is higher for alumina ceramics sintered in the hybrid microwave kiln (MK-Al_2O_3) than in the electric kiln (EK-Al_2O_3).
- The brittleness index (B_i, $\mu m^{-1/2}$) is higher for alumina ceramics sintered in the electric kiln (EK-Al_2O_3) than in the hybrid microwave kiln (MK-Al_2O_3).
- Both Vickers hardness and brittleness index values might be correlated to the microstructure of sintered samples.
- Non-conventionally sintered alumina samples have higher hardness and lower brittleness index probably due to the finer microstructure.

Acknowledgements

This work has been fully supported by the Croatian Science Foundation under the project IP-2016-06-6000: "Monolithic and composite advanced ceramics for wear and corrosion protection" (WECOR).

References

[1] Lóh, N.J., Simão, L., Jiusti, J., De Noni Jr., A., Montedo, O.R.K., Effect of temperature and holding time on the densification of alumina obtained by two-step sintering, *Ceram Int*, 43 (11), 8269–8275 (2017).

[2] Tian, Q., Dai, J., Xu, L., Wang, X., Advance of Sintering Methods of High Purity Alumina Ceramics, *Key Engineering Materials*, 703, 76–80 (2016).

[3] Figiel, P., Rozmus, M., Smuk, B., Properties of alumina ceramics obtained by conventional and non-conventional methods for sintering ceramics, *Journal of Achievements in Materials and Manufacturing Engineering*, 48 (1), 29–34 (2011).

[4] Agrawal, D., Microwave sintering of ceramics, composites and metal powders, in Sintering of Advanced Materials, Woodhead Publishing, 222–248 (2010).

[5] Ćurković, L., Veseli, R., Gabelica, I., Žmak, I., Ropuš, I., Vukšić, M., A review of microwave-assisted sintering technique, *Transactions of Famena*, 45, 1–12 (2021).

[6] Borrell, A., Salvador, MD., Advanced Ceramic Materials Sintered by Microwave Technology, In: IntechOpen., 2018.

[7] Orlik, K., Lorgouilloux, Y., Marchet, P., Thuault, A., Rguiti, M., Courtois, C., Jean, F., Influence of microwave sintering on electrical properties of BCTZ lead free piezoelectric ceramics, *J Eur Ceram Soc*, 40(4), 1212–1216 (2020).

[8] Liu, Y., Zhu, J., Dai, B., Transparent $MgAl_2O_4$ ceramics prepared by microwave sintering and hot isostatic pressing, *Ceram Int*, 46(16), 25738–25740 (2020).

[9] Ramesh, S., Zulkifli, N., Tan, CY., Wong, Y.H., Tarlochan, F., Ramesh, S., Teng, W.D., Sopyan, I., Bang, L.T., Sarhan, A.A.D., Comparison between microwave and conventional sintering on the properties and microstructural evolution of tetragonal zirconia, *Ceram Int*, 44(8), 8922–8927 (2018).

[10] Chen, Y., Fan, B., Yang, B., Ma, W., Liu, G., Li, H., Microwave sintering and fracture behavior of zirconia ceramics, *Ceram Int*, 45(14), 17675–17680 (2019).

[11] Croquesel, J., Carry, CP., Chaix, JM., Bouvard, D., Saunier, S., Direct microwave sintering of alumina in a single mode cavity: Magnesium doping effects, *J Eur Ceram Soc*, 38(4), 1841–1845 (2018).

[12] Shukla, M., Ghosh, S., Dandapat, N., Mandal, AK., Balla, VK., Comparative Study on Conventional Sintering with Microwave Sintering and Vacuum Sintering of Y_2O_2-Al_2O_3-ZrO_2 Ceramics, *Journal of Materials Science and Chemical Engineering*, 4(2), 71–78 (2016).

[13] Curto, H., Thuault, A., Jean, F., Violier, M., Dupont, V., Hornez, J.H., Leriche, A., Coupling additive manufacturing and microwave sintering: A fast processing route of alumina ceramics, *J Eur Ceram Soc*, 40(7), 2548-2554 (2020).

[14] Zhan, H., Zhang, N., Wu, D., Wu, Z., Bi, S., Ma., B, Liu, W., Controlled synthesis of β-SiC with a novel microwave sintering method, *Materials Letters*, 25, 126586 (2019).

[15] Tao, S.C., Xu, J.L., Yuan, L., Luo, J.M., Zheng, YF., Microstructure, mechanical properties and antibacterial properties of the microwave sintered porous Ti–3Cu alloys, *J Alloys Compd*, 812, 1–9 (2020).

[16] Nagaraju, K.V.V., Kumaran, S., Srinivasa Rao, T., Microwave sintering of 316L stainless steel: Influence of sintering temperature and time, *Materials Today: Proceedings*, 27(3), 2066–2071 (2020).

[17] Sethi, G., Upadhyaya, A., Agrawal, D., Microwave and Conventional Sintering of Premixed and Prealloyed Cu-12Sn Bronze, *Science of sintering*, 35, 49–65 (2003).

[18] Wang, L., Guo, S., Gao, J. et al., Microwave sintering behavior of FeCuCo based metallic powder for diamond alloy tool bit, *J Alloys Compd*, 727, 94–99 (2017).

[19] Madhan, M., Prabhakaran, G., Microwave versus conventional sintering: Microstructure and mechanical properties of Al_2O_3-SiC ceramic composites, *Boletin de la Sociedad Espanola de Ceramica y Vidrio*, 58(1), 14–22 (2019).

[20] Wei, C., Xu, X., Wei, B., Cheng, J., Chen, P., Effect of diamond surface treatment on microstructure and thermal conductivity of diamond/W-30Cu composites prepared by microwave sintering, *Diamond and Related Materials*, 104, 107760 (2020).

[21] Gil-Flores, L., Salvador, MD., Penaranda-Foix, FL. et al., Microstructure and mechanical properties of 5.8 GHz microwave-sintered ZrO_2/Al_2O_3 ceramics, *Ceram Int*, 45(14), 18059–18064 (2019).

[22] Peng, Q., Tang, Z., Wang, Y., Peng, Z., Mechanical performance and in-vitro biological behaviors of boronized Ti6Al4V/HA composites synthesized by microwave sintering, *Ceram Int*, 45(18), 24684–24690 (2019).

[23] Ćurković, L., Lalić, M., Šolić, S., Analysis of the indentation size effect on the hardness of alumina ceramics using different models, *Kov Mater*, 47 (2) 89–93 (2009).

[24] Bhattacharya, S., Kundu, R., Bhattacharya, K., Poddar, A., Roy, D. Micromechanical hardness study and the effect of reverse indentation size on heat-treated silver doped zinc-molybdate glass nanocomposites, *J Alloys Compd*, 770, 136–142 (2019).

[25] Kampouris, A.K., Konstantinidis, A.A., On the interpretation of the indentation size effect (ISE) through gradient theory for Vickers and Berkovich, *Journal of the Mechanical Behavior of Materials*, 25 (5–6), 161–164 (2017).

[26] Pharr, G.M., Herbert, E.G., Gao, Y., The indentation size effect: A critical examination of experimental observations and mechanistic interpretations, *Annual Review of Materials Research*, 40, 271–292 (2010).

[27] Peng, Z., Gong, J., Miao, H., On the description of indentation size effect in hardness testing for ceramics: Analysis of the nanoindentation data, *J Eur Ceram Soc*, 24, 2193–2201 (2004).

[28] Majić Renjo, M., Ćurković, L., Štefančić, S., Ćorić, D., Indentation size effect of Y-TZP dental ceramics. *Dent Mater*, 30 (12), e371–e376 (2014).

[29] Majić Renjo, M., Rede, V., Ćurković, L., Reverse indentation size effect of a duplex steel, Kov Mater, 52(5), 299-304 (2014).

[30] Menezes, R.R., Souto P.M., Kiminami, R.H.G.A., Microwave Fast Sintering of Ceramic Materials, In book: Sintering of Ceramics - New Emerging Techniques Edited by Arunachalam Lakshmanan, IntechOpen, 2012.

[31] Žmak, I., Ćorić, D., Mandić, V., Ćurković, L., Hardness and Indentation Fracture Toughness of Slip Cast Alumina and Alumina-Zirconia Ceramics, *Materials*, 13, 1–17 (2020).

[32] Chinn RE., Ceramography, Preparation and Analysis of Ceramic Microstructure. Materials Park: ASM International, 2002.

[33] Moraes, M.C.C., Elias, C.N., Mechanical properties of alumina-zirconia composites for ceramic abutments, *Mat Res*, 7(4), 643–649 (2004).

[34] Gong, J., Wu, J., Guan, Z., Analysis of the indentation size effect on the apparent hardness for ceramics, *Materials Letters*, 38, 197–201 (1999).

[36] Li, H., Bradt, R.C., The microhardness indentation load/size effect in rutile and cassiterite single crystals, *J Mater Sci*, 28, 917–926 (1993).

[37] Gong. J., Guan. Z., Load dependence of low-load Knoophardness in ceramics: a modified PSR model. *Mater Lett*, 47, 140–144 (2001).

[38] Montgomery, D.C. Design and Analysis of Experiments. John Wiley & Sons, Inc., 2013.

[39] Elsaka, S.E., Elnaghy, A.M., Mechanical properties of zirconia reinforced lithium silicate glass-ceramic, *Dent Mater*, 32, 908–914 (2016).